Open-boundary cluster model for calculation of adsorbate-surface electronic states

Tomokazu Yasuike and Katsuyuki Nobusada*
Department of Theoretical and Computational Molecular Science, Institute for Molecular Science, Myodaiji, Okazaki, Aichi 444-8585, Japan
and Department of Structural Molecular Science, School of Physical Sciences, The Graduate University for Advanced Studies (SOKENDAI), Myodaiji, Okazaki, Aichi 444-8585, Japan
(Received 20 July 2007; published 3 December 2007)

We have developed a simple embedded-cluster model approach to investigate adsorbate-surface systems. In our approach, the physically relevant subsystem is described as an open-quantum system by considering a model cluster subject to an outgoing-wave boundary condition at the edge. This open-boundary cluster model (OCM) is free from artificial waves reflected at the cluster edge, and thus the adsorbate properties computed with the OCM are almost independent of the model cluster size. The exact continuous density of states (DOS) of a one-dimensional periodic potential model is shown to be precisely reproduced with the OCM. The accurate DOS leads to an appropriate description of adsorbate-surface chemical bonding. Moreover, the open-boundary treatment of the OCM allows us to evaluate the electron-transfer rate from the adsorbate to the surface, whereas the conventional cluster model does not give any information about such a dynamical process.

DOI: 10.1103/PhysRevB.76.235401 PACS number(s): 73.20.Hb, 33.35.+r, 34.50.Dy, 79.20.La

I. INTRODUCTION

Adsorbate-surface systems have been receiving considerable attention over the years because of their importance in heterogeneous catalysis and corrosion.[1] It has nevertheless been difficult to experimentally investigate adsorbate molecular processes on surfaces through specifying adsorption sites and internal states. In the early days, the adsorption studies were carried out on adsorbent surfaces of largely unknown compositions and structure. Although characterization technique of surfaces had greatly been improved with the advances of field-ion microscopy, field-electron microscopy, and low-energy electron diffraction,[2] no direct microscopic information on the adsorption had been obtained until the invention of the scanning tunneling microscopy (STM) in 1982.[3] The local probe by means of the STM enables us to observe site-dependent vibrational spectra and to reveal dynamics of adsorbates on surfaces.[4–6] In addition to the STM, the femtosecond time-resolved spectroscopy also came into being in the 1980s. The real-time observation of photoinduced adsorbate dynamics such as coherent motion of nuclei and its decoherence[7–9] has been realized. This experimental progress is now advancing chemical physics of adsorbate-surface systems toward the exact science, and this movement requires a theoretical model to quantitatively describe the nature of their electronic states at a currently available computational cost. Our aim in the present paper is to propose a simple method giving not only shapes of potential energy surfaces but also rates of electron decay from adsorbates to metallic surfaces. It should be noted that the electronic lifetime is a crucial parameter in surface physics and chemistry, since photophysical and photochemical properties at surfaces depend on the electron decay processes as well as the reactivity of electronically excited states.

The previous theoretical methods for investigating electronic states of adsorbate-surface systems can be classified into three categories.[10] In the solid state physics, the slab-supercell approach[11–20] has conventionally been employed because of easy implementation with available energy-band computational codes. In this approach, the surface is replaced by a two-dimensional (2D) periodic slab having a finite thickness, and the slabs are repeated by adding a vacuum region between them to recover the three-dimensional periodicity needed for the band calculation. Whereas the infiniteness in the direction parallel to the surface is appropriately taken into account, the semi-infiniteness in the direction normal to the surface is lost by the artificial geometry introduced in the supercell calculation. Moreover, when we study a single molecule interacting with a metal surface or a low coverage surface, the size of the unit cell must be taken as large as the lateral interactions between adsorbates in the 2D periodic slab are negligible. For such cases, the computational cost becomes highly expensive.

On the other hand, quantum chemists have been employing the cluster model approach.[21–27] In this approach, an adsorbate-surface system is mimicked by a model cluster consisting of an adsorbate and a subsystem carved out from a bulk surface. This approach is conceptually simple and is expected to lower computational costs if a surface is reasonably modeled by clusters with fewer atoms. Moreover, all the electronic structure theories developed for molecules are straightforwardly applicable to the adsorbate-surface model cluster, and thus even electronic excited states can easily be obtained with many-body formalisms such as a configuration interaction method. This conventional cluster model (CCM) approach has been successful in studying chemisorption of atoms and molecules on covalent Si surfaces.[25–27] However, ignorance of the interaction between the subsystem and environments is known to cause serious problems: (1) computed physical properties depend on the size of the model cluster, (2) continuous band structures in density of states are not reproduced, and (3) lifetimes of electron decay from adsorbates to metallic surfaces cannot be obtained.

While the naive CCM approach has these disadvantages, the concept of the cluster model which describes the physically relevant subsystem of the adsorbate-surface systems is not only intuitive but also effective from the viewpoint of the

computational cost. For this reason, generalizations of the CCM have so far been explored extensively to describe the cluster model interacting with environments.[28–39] Such generalized methods are collectively called the embedded-cluster approach. The most simple one is a model cluster embedded in a background of classical point charges.[28–30] It may provide a reasonable description for ionic surfaces in which the electronic states are localized. More sophisticated methods for constructing effective embedding potentials have been developed on the basis of a localization transformation in orbital space[32–35] or of an electron density partition in the density-functional theory.[36–39] The periodic density-functional embedding theory by Carter and co-workers[37–39] has been developed to handle an adsorption on metallic surfaces and has been shown to predict correct geometries and vertical excitation energies of the adsorption of CO on Pd(111).[39] However, the effects originating from the continuous energy spectra of the semi-infinite surfaces cannot be taken into account with these types of the embedding because they do not appropriately handle the boundary condition of the wave function in the model cluster. As will be described later, according to the Löwdin-Feshbach theory,[40,41] the physically relevant subsystem (i.e., the model cluster) should generally be extracted as not an isolated but an open-quantum system. In the above embedded-cluster methods, the model cluster is basically treated as an isolated quantum system. Although a few of them partially include the effects of an open system on the basis of formalism of fractional occupation number,[31,35] they are still insufficient.

More promising might be the method based on a general partitioning procedure such as the Löwdin-Feshbach theory. This kind of the embedding scheme has been implemented with the Dyson equation for the Green functions[42–44] and Green function matching at the interface between a model cluster and environments,[45,46] and their validity has been proved.[10] Nevertheless, the approach has not been employed intensively because its practical implementation is somewhat complicated and the computational cost is much more expensive than that required in the CCM or the simpler embedded-cluster models.

In the present paper, we propose an alternative simple method of the embedded-cluster model to treat electronic states of an adsorbate-surface system by using the complex-scaling technique.[47] While its effectiveness for adsorbate nuclear motions on surfaces has been proved by Moiseyev *et al.*,[48] only few attempts have so far been made at the application to electronic degrees of freedom. Nordlander and Tully have applied the complex-scaling technique[49,50] to an atomic adsorption on a jellium surface and have successfully obtained the excited resonance one-body levels of the adatom. Their atom-jellium modeling of the adsorbate-surface system, however, was not able to describe any chemisorptive bonds. We will show in the present paper that the complex-scaled cluster model can describe both of resonant levels and chemisorptive bonds. Our approach is equivalent to a procedure in which the outgoing-wave boundary condition (OBC) is imposed on the edge of the model cluster, and thus, we refer to this approach as the open-boundary cluster model (OCM).

The paper is organized as follows. Section II explains the OCM approach and shows that the OCM approach reasonably reproduces the exact continuous density of states (DOS) for a one-dimensional periodic crystal model. In Sec. III, the OCM approach is applied to an adsorbate-surface model system, and we clarify the OBC effect on chemical bond by utilizing the real-space one-body reduced density matrix (1-RDM). In Sec. IV, we furthermore demonstrate electronic-excitation effects on the adsorption energy and the rate of the electron transfer from the adsorbate to the surface. We discuss the applicability of the OCM to the *ab initio* Hamiltonians in Sec. V. Concluding remarks are presented in Sec. VI.

II. OPEN-BOUNDARY CLUSTER MODEL

A. Extraction of subsystem in quantum mechanics

The common heart of all the cluster model approaches is an extraction of a physically relevant subsystem from the whole adsorbate-surface system. In the quantum mechanics, the extraction of a subsystem is formally carried out with the complementary projection operators P and $Q \equiv 1-P$. Under the conditions that the initial wave function has only P space components and the energy of the initial state is well defined, the Löwdin-Feshbach theory[40,41,51,52] shows that the time-dependent Schrödinger equation for $P\psi$ is given by

$$P\dot{\psi}(t) = H_{\text{eff}}^{P}(E)P\psi, \tag{1}$$

where $H_{\text{eff}}^{P}(E)$ is an energy-dependent effective Hamiltonian,

$$H_{\text{eff}}^{P}(E) = PHP + PHQ\frac{1}{E - QHQ + i\epsilon}QHP \tag{2a}$$

$$\xrightarrow{\epsilon\to 0} PHP + PHQ\left[\mathcal{P}\frac{1}{E - QHQ} + i\pi\delta(E - QHQ)\right]QHP \tag{2b}$$

$$= PHP + \Delta(E) - \frac{i}{2}\Gamma(E). \tag{2c}$$

The symbol $\mathcal{P}$ in Eq. (2b) denotes the Cauchy principal value. The second and third terms in the right-hand side of Eq. (2c) represent the interaction between the subsystem and the environment and cause the energy shift and the dissipation, respectively, for the PHP eigenstates. This equation clearly shows that the subsystem should be extracted as an open-quantum system. In the CCM, only the term of PHP is taken into account in the model Hamiltonian. Many embedding methods have so far been developed to phenomenologically include the effects of the remaining terms of $\Delta(E)$ and $\Gamma(E)$. The simple embedding methods using point charges[28–30] or effective embedding potentials[32–39] generally avoid directly calculating the surface Green function,

$$G_{QQ}^{\dagger}(E) \equiv \frac{1}{E - QHQ + i\epsilon}, \tag{3}$$

and are built up to include only the energy-shift effect due to the electrostatic interaction with the background environment. This kind of the embedding method is not applicable

to the processes accompanied by decay of electronic states. More sophisticated methods are directly based on the Löwdin-Feshbach partitioning of the total Green function and have been considered to be the most accurate cluster-based methods having a sound theoretical foundation.[10,42,43,45,46] Nevertheless, they have not been employed intensively because their practical implementation is somewhat complicated and cumbersome.[10] The computation of the surface Green function $G^{\dagger}_{QQ}(E)$ is demanding, and the resultant energy-dependent effective Hamiltonian $H^P_{\mathrm{eff}}(E)$ causes other difficulties as follows. The eigenvalue problem for $H^P_{\mathrm{eff}}(E)$ has to be formulated with an auxiliary fixed-point equation,

$$H^P_{\mathrm{eff}}(E)\Psi_i(E) = \tilde{E}_i(E)\Psi_i(E), \tag{4}$$

$$\mathrm{Re}[\tilde{E}_i(E)] = E. \tag{5}$$

In addition, the numerical integration over the energy is needed to calculate physical properties. For instance, the one-electron density $\rho(r)$ is obtained from

$$\rho(r) = \frac{1}{\pi}\,\mathrm{Im}\int_{-\infty}^{E_F}\mathrm{Tr}\left[\frac{1}{E - H^P_{\mathrm{eff}}(E)}\right]dE. \tag{6}$$

It should also be noted that the completeness and the orthonormality of the eigenfunctions are satisfied only among the eigenfunctions for the same E.

In nuclear theory, the formalisms based on the energy-dependent effective Hamiltonian have extensively been investigated,[53] and the resonance approximations to them have been discussed for a long time.[54–56] In the resonance approximation, the energy dependence of $H^P_{\mathrm{eff}}(E)$ is neglected, and the effective Hamiltonian $H^P_{\mathrm{eff}}(E)$ is recast into the form of an effective resonant Hamiltonian H^P_{res},

$$H^P_{\mathrm{res}} = PHP + \Delta - i\frac{\Gamma}{2}. \tag{7}$$

At this level of description, the dynamics in the P space is expressed by a superposition of the eigenstates of the non-Hermitian resonant Hamiltonian H^P_{res}. These eigenstates are resonance states with complex eigenvalues,

$$E_n = \epsilon_n - i\gamma_n/2, \tag{8}$$

where ϵ_n is the resonance position and γ_n is the inverse lifetime of each state. As Weisskopf and Wigner have shown,[57] the resonant Hamiltonian approximation is justified when the QHQ continuous spectrum is dense and the energy dependence of PHQ and QHP can be neglected. It has been shown in the Humblet-Rosenfeld theory of nuclear reaction[54] that the resonance modeling of the effective Hamiltonian is appropriately carried out by using the Siegert states.[58] In the present study, we employ the Siegert-state representation of the effective resonance Hamiltonian as a simple embedding method for adsorbate-surface systems. In this approach, we can obtain the resonance states of H^P_{res} as the Siegert states without the knowledge of Δ and Γ. The Siegert states are alternatively obtained by the introduction of the OBC at the edge of the model cluster Hamiltonian, PHP. They are known to have complex eigenvalues and to satisfy the OBC in the asymptotic region. Unlike the boundary condition for the bound states, the OBC is suitable for describing dissipation in the asymptotic region. The extraction of the relevant subsystem using the resonant effective Hamiltonian neglects the detailed structure of the QHQ spectrum, and the validity of this procedure will be confirmed numerically.

As shown later, owing to the introduction of the OBC, a continuous density of states of a bulk crystal is successfully reproduced. This feature of the OCM is expected to redeem the drawbacks of the CCM. On the other hand, the introduction of the OBC gives rise to a numerical problem that we must deal with the Siegert wave functions diverging exponentially in the asymptotic region. However, the problem can be safely circumvented by complex scaling of the model Hamiltonian.[47,59,60] In the following section, we describe the complex-scaling technique necessary for calculating the Siegert states.

B. Complex-scaling technique

The asymptotic form of the resonance wave function $\psi^n_{\mathrm{res}}(x)$ is given by

$$\psi^n_{\mathrm{res}}(x) \sim \exp[i(k'_n - ik''_n)x] = \exp[ik'_n x]\exp[+k''_n x], \tag{9}$$

where k'_n and k''_n are defined as $\mathrm{Re}[\sqrt{2E_n}]$ and $-\mathrm{Im}[\sqrt{2E_n}]$, respectively. These variables have positive real values because the resonance poles arise in the second sheet of the complex-energy Riemann surface. The resonance wave function diverges exponentially at $x\to\infty$ due to the last term of Eq. (9), $e^{k''_n x}$. The asymptotic form of the complex-scaled resonant wave function $\psi_{\mathrm{res}}(xe^{i\theta})$ is written in the form of

$$\begin{aligned}\psi^n_{\mathrm{res}}(xe^{i\theta}) &\sim \exp[i(k'_n - ik''_n)xe^{i\theta}] \\ &= \exp[i(k'_n\cos\theta + k''_n\sin\theta)x] \\ &\quad\times\exp[(k''_n\cos\theta - k'_n\sin\theta)x].\end{aligned} \tag{10}$$

If $k''_n/k'_n < \tan\theta$, the resonance wave function becomes an L^2 function. The rotation angle θ controls the size of the wave function. On the other hand, any rotation angle satisfying $k''_n/k'_n < \tan\theta$ gives the same eigenvalues for usual resonance states in isolated atomic and molecular systems, and thus, the choice of θ is not so important in the limit of the complete basis set.[47] However, this is not necessarily true when the complex-scaling method is applied to the extraction of a subsystem from delocalized systems such as crystals and adsorbate-surface systems. One can control the size of model clusters by changing the rotation angle θ. The continuous change of θ is possible, but its local appropriate value should be specified by the complex variational principle.[47] This procedure will be explicitly explained through the numerical results in the next section.

C. Density of states for one-dimensional bulk crystal

To demonstrate that the OCM reasonably reproduces a continuous energy spectrum of a surface, we first introduce a numerical model of a one-dimensional bulk crystal defined by the following one-body Hamiltonian $H_0(x)$,

$$H_0(x) = -\frac{1}{2}\frac{d^2}{dx^2} - \sum_{l=-L}^{L} \frac{2}{\cosh^2(x-la)}, \tag{11}$$

where $2L+1$ is the number of the atomic site, x indicates the electron coordinate, and the lattice constant a is set to be 3.0. We employ this simple model because the aim of the present work is to show how the OCM approach works as a first step toward the development of the alternative embedded-cluster model rather than to solve a specific problem in an adsorbate-surface system. The one-body energy spectrum of the CCM $\{E_n^{\mathrm{CCM}}\}$ is obtained by diagonalizing the Hamiltonian matrix $\mathbf{H}_0(x)$ represented with a certain basis set. In the present study, we used the equally spaced grid representation by Colbert and Miller.[61] The one-body DOS $\rho(E)$ is generally defined as

$$\rho(E) = -\frac{1}{\pi}\mathrm{Tr}\left[\mathrm{Im}\,\frac{1}{E - H_0 + i\epsilon}\right], \tag{12}$$

and then, the one-body DOS for the CCM, $\rho_{\mathrm{CCM}}(E)$, is

$$\rho_{\mathrm{CCM}}(E) = \sum_n \delta(E - E_n^{\mathrm{CCM}}). \tag{13}$$

In the limit of $L \to \infty$, the eigenfunctions of the system are expanded in terms of the Bloch waves. By using the basis set defined as

$$\phi_{k,n}(x) = \frac{1}{\sqrt{2\pi}} e^{i(k+h_n)x} \quad \left(h_n = n\frac{2\pi}{a}\right), \tag{14}$$

the matrix elements of Hamiltonian H^k_{crystal} are given by

$$\mathrm{H}^k_{\mathrm{crystal}_{mn}} \equiv \langle \phi_{k,m}|H|\phi_{k,n}\rangle = \frac{(k+h_n)^2}{2}\delta_{mn} + \tilde{V}(h_m - h_n), \tag{15}$$

where $\tilde{V}$ is the Fourier transformation of the potential energy-function. An energy-band structure is obtained by diagonalizing H^k_{crystal} repeatedly for given values of k. The corresponding one-body DOS, $\rho_{\mathrm{crystal}}(E)$, is calculated by

$$\rho_{\mathrm{crystal}}(E) = \left(\frac{dE(k)}{dk}\right)^{-1}. \tag{16}$$

The OCM one-body energy spectrum is obtained by diagonalizing the complex-scaled Hamiltonian matrix $\mathbf{H}_0(xe^{i\theta})$. The rotation angle θ is determined on the basis of the complex variational principle. The OCM eigenstates have the complex eigenvalues $\{E_n^{\mathrm{OCM}} = \epsilon_n - i\gamma_n/2\}$. By using Eq. (12), the one-body DOS for the OCM is written as

$$\rho_{\mathrm{OCM}}(E) = \frac{1}{\pi}\sum_n \frac{\gamma_n/2}{(E-\epsilon_n)^2 + (\gamma_n/2)^2}. \tag{17}$$

Figure 1 shows a part of the energy spectrum and the representative wave functions for the OCM at (a) θ=2.00 and (b) θ=2.95. As mentioned above, the wave functions are found to be more localized at a larger rotation angle. In both the cases of θ=2.00 and 2.95, the complex variational principle is satisfied, and the general shapes of the energy spectra on the complex E plane resemble each other except that the number of constituents is different. This implies that the OCM qualitatively gives the same properties, irrespective of the cluster size.

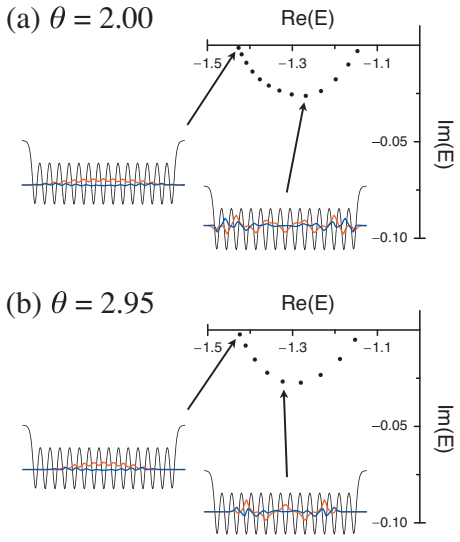

FIG. 1. (Color) Energy spectra and representative wave functions for the OCM Hamiltonian with L=7: (a) θ=2.00 and (b) θ=2.95. The real and imaginary parts of the wave functions are indicated by red and blue colors, respectively.

Figure 2 shows the calculated DOSs for the CCM (gray), the perfect one-dimensional crystal (red), and the OCM (L=7) at θ=2.00 (blue) and 2.95 (green). Unlike the CCM-DOS, the OCM-DOSs are continuous functions of energy and well reproduce the crystal DOS. As expected, the DOSs calculated at θ=2.00 and 2.95 closely resemble each other, and the OCM qualitatively gives physical properties independent of the cluster size. Of course, the DOS obtained at the smaller θ gives the better agreement with the exact DOS because the larger spatial region is included in the model, as shown in Fig. 1(a). The preliminary calculation for L=6 showed that the scaling angle θ=2.95 was the smallest value that satisfies the complex variational principle. We have con-

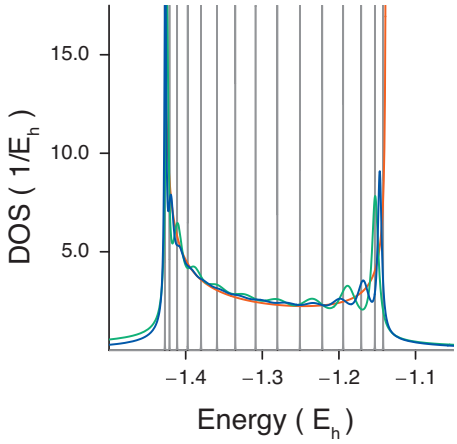

FIG. 2. (Color) Comparison of the one-electron density of states (DOS) obtained with the CCM [the gray-colored array of δ functions: Eq. (13)], the OCM [θ=2.00 (blue), 2.95 (green): Eq. (17)], and the exact band calculation [(red): Eq. (16)].

firmed that the DOS calculated for $L=6$ and $\theta=2.95$ completely agrees with that for $L=7$ and $\theta=2.95$. This means that the effective cluster size of the OCM depends not only on the number of the atomic site L but also on the scaling angle θ. The above observations lead to the conclusion that the smallest θ satisfying the complex variational principle should be used for a given Hamiltonian.

In the CCM approach, the discrete energy levels are often convoluted by the Gaussian function having an assumed width for comparison with the bulk DOS.[62,63] However, such a convolution cannot reproduce the spectral features that the crystal DOS diverges at the edge of the band and is smooth around the middle of the band. In contrast, as shown in Fig. 2, the OCM calculation automatically gives the reasonable linewidths depending on each energy level. Figure 1 shows that the imaginary part of the eigenvalue γ_n is very small at the edge of the energy spectra, $\mathrm{Re}(E_n)\sim -1.4$. This is ascribed to the fact that the corresponding wave function has only a small value at the end of the cluster. On the other hand, the eigenfunction with the energy around the middle of the energy spectra, i.e., $\mathrm{Re}(E_n)\sim -1.3$, has a large value at the end of the cluster, and thus γ_n becomes large. This behavior of the energy widths leads to the well reproduction of the above-mentioned feature in Fig. 2.

D. Advantage of open-boundary cluster model and relationship to the work of Nordlander and Tully

As shown in the last section, the OCM approach gives an appropriate estimate of the DOS for the bulk crystal only by diagonalizing the complex-scaled CCM Hamiltonian. The extra cost needed for the OCM computation is not expensive, and thus, the approach is promising for a first-principles modeling of adsorbate-surface systems. Other embedded-cluster approaches which give a correct DOS are computationally much more demanding because of the use of the energy-dependent effective Hamiltonian, as described in Sec. II A. Such methods require different self-consistent computations at all the energies in the energy range in which one wants to know the DOS, whereas the OCM approach needs only a single diagonalization to obtain the DOS over the whole energy range. The DOS is constructed by using the computed eigenvalues and Eq. (17).

The advantage of the OCM over the slab-supercell approach is more noteworthy. The slab-supercell calculation does not necessarily provide a reasonable description for adsorbate-surface systems owing to the inaccurate boundary condition in the direction normal to the surface and is nevertheless computationally demanding because it is based on energy-band calculation in which the k-point sampling is needed.

Nordlander and Tully have applied the complex-scaling technique to describe the resonance formation in adsorbate-surface model systems.[49,50] They have employed a jellium model[64] to represent a surface. The complex-scaling technique has been used to obtain the resonance levels derived from the interaction between the adsorbate discrete levels and the continuum states in the semi-infinite jellium surface. In the present work, we propose that the application of the complex-scaling technique to a model cluster naturally gives an open-system treatment of the cluster along the spirit of the Löwdin-Feshbach partitioning theory. The point to be stressed is that no explicit attention to the modeling of the semi-infinite surface is needed to be paid in the OCM approach, unlike the jellium surface which has to be specified by a value of the average electron density. On the other hand, it is also true that the OCM has a close relationship to the modeling of Nordlander and Tully in some sense. To manifest it, we now consider the system described by the one-body Hamiltonian,

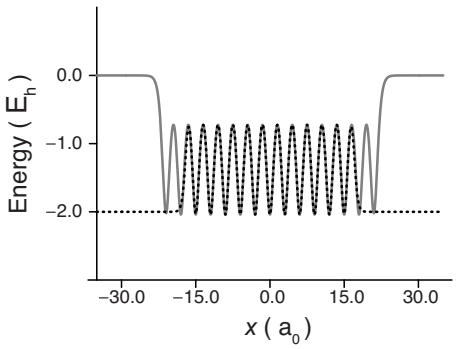

FIG. 3. Comparison of the potential terms in the employed Hamiltonians of Eq. (11) (gray-bold curve) and Eq. (18) (black-dotted curve).

$$H_0(x) = -\frac{1}{2}\frac{d^2}{dx^2} - \sum_{l=-5}^{5}\frac{2}{\cosh^2(x-la)} - \frac{2}{1+e^{2.75(x+17)}} - \frac{2}{1+e^{-2.75(x-17)}}. \tag{18}$$

Figure 3 shows the potential part of this Hamiltonian (the black-dotted curve) in comparison with the potential of the OCM (the gray-bold curve). The black-dotted curve shows that the model system consists of the cluster including 11 atoms and of the jelliumlike potentials which are smoothly connected to both edges of the cluster. Namely, the above Hamiltonian of Eq. (18) represents the cluster embedded in the jellium surface. The resonance states in this system are obtained by the complex-scaling technique as Nordlander and Tully have done. When the scaling parameter θ is set to be 2.95, the complex variational principle is satisfied. The DOS of the jellium surface model is in complete agreement with the DOS obtained with the OCM Hamiltonian at $\theta=2.95$ in the energy range of $E=-1.5$ to -1.1. This equivalence between these two modelings is due to the fact that the OCM wave functions for $\theta=2.95$, shown in Fig. 1(b), are localized in the center 11-atom region. Therefore, the model cluster in the OCM approach could be regarded as a jellium-embedded cluster. The model cluster implicitly embedded in the jellium includes not only the adsorbate but also the surface atoms, and thus, it is a generalization of the treatment of Nordlander and Tully, in which the adsorbate is directly embedded in the jellium surface. It should be noted that the effects derived from the smoothly connected jellium are included without explicitly including the jellium potential in

the OCM Hamiltonian. This OCM preferable nature is a consequence from the known fact that determination of resonance wave functions does not require any information about the asymptotic continuum wave functions. The simplicity of the OCM is based on the general local nature of the resonance wave functions.

III. ADSORPTION PROBLEM WITH OPEN-BOUNDARY CLUSTER MODEL

A. Definition of Hamiltonian and local quantities

In this section, we discuss an atomic adsorption on a surface with the OCM. The employed one-body, one-dimensional model Hamiltonian is

$$H_0(x,R) = -\frac{1}{2}\frac{d^2}{dx^2} - \sum_{l=0}^{10} \frac{2}{\cosh^2(x+la)} - \frac{4.55}{\cosh^2(x-R)}, \tag{19}$$

where R is the distance between the adsorbate atom and the surface, and the lattice constant a is set equal to 3.0. It is convenient for the adsorbate-surface system to introduce local quantities such as local density of states and local energy. The key concept for defining the local quantities is a partial trace of a projection operator on a subspace. For a Hermitian Hamiltonian, the projection operator on the ψ_n one-body state is written as $|\psi_n\rangle\langle\psi_n|$ by using the usual inner product, and the partial trace of it on the subspace A becomes

$$\mathrm{Tr}_A[|\psi_n\rangle\langle\psi_n|] = \int_{x\subset A} |\psi_n(x)|^2 dx = 1 - \int_{x\not\subset A} |\psi_n(x)|^2 dx \leq 1. \tag{20}$$

This equation shows that $\mathrm{Tr}_A[|\psi_n\rangle\langle\psi_n|]$ has a physical meaning as the weight of the ψ_n state in the subspace A. In the OCM, the c-product formalism should alternatively be used because a Hamiltonian matrix becomes complex symmetric by the complex-scaling transformation. In this formalism, the complex conjugation is not applied to the bra state in the inner product. This definition is called c product and indicated with the round bracket. The projection operator is then given by $|\psi_n)(\psi_n|$, and the partial trace on the subspace A in the form of

$$\mathrm{Tr}_A[|\psi_n)(\psi_n|] = \int_{x\subset A} \psi_n^2(x) dx \tag{21}$$

becomes a complex value. According to Berggren, the real and imaginary parts of the trace can be interpreted as the average and the uncertainty of the weight, respectively.[65] We thus follow the Berggren's interpretation and define the local quantity of the weight by carrying out the substitution,

$$\mathrm{Tr}_A[|\psi_n)(\psi_n|] \to \mathrm{Re}(\mathrm{Tr}_A[|\psi_n)(\psi_n|]) \equiv w_n^A. \tag{22}$$

Then, the one-body local density of states (LDOS) is given by

$$\rho_{\mathrm{OCM}}^A(E) = -\frac{1}{\pi}\mathrm{Tr}_A\left[\mathrm{Im}\frac{1}{E-H_0+i\epsilon}\right] = -\frac{1}{\pi}\mathrm{Im}\,\mathrm{Tr}_A\left[\sum_n \frac{|\psi_n)(\psi_n|}{E-E_n^{\mathrm{OCM}}}\right] \tag{23}$$

$$\to -\frac{1}{\pi}\mathrm{Im}\sum_n \frac{w_n^A}{E-E_n^{\mathrm{OCM}}} = \frac{1}{\pi}\sum_n \frac{w_n^A(\gamma_n/2)}{(E-\epsilon_n)^2+(\gamma_n/2)^2}. \tag{24}$$

To discuss adsorption energy and local adsorption energy, we consider the many-body Hamiltonian,

$$H = \sum_j H_0(x_j,R), \tag{25}$$

where H_0 is the one-body Hamiltonian [Eq. (19)] and x_j is the jth electron coordinate. This many-body Hamiltonian has only one-body terms in the end, and thus, the expectation value of the Hamiltonian is easily obtained by

$$\langle H\rangle = \mathrm{Tr}[H_0\rho], \tag{26}$$

where ρ is the equilibrium 1-RDM. By using the one-body eigenstate representation, H_0 and ρ are expressed by

$$H_0 = \sum_n |\psi_n) E_n^{\mathrm{OCM}} (\psi_n|, \tag{27}$$

and

$$\rho = \sum_n |\psi_n) f_n(\mu) (\psi_n|, \tag{28}$$

respectively, where $f_n(\mu)$ is the occupation number of the state ψ_n for a system having a chemical potential μ,

$$f_n(\mu) \equiv \frac{2}{\pi}\int_{-\infty}^{\mu} dE \frac{\gamma_n/2}{(E-\epsilon_n)^2+(\gamma_n/2)^2}. \tag{29}$$

This expression allows us to use fractional occupation numbers, which are attributed to the open-system character of the present model. The total energy of the system is given by

$$\langle E\rangle \equiv \mathrm{Tr}[H_0\rho] = \mathrm{Tr}\left[\sum_n |\psi_n) f_n(\mu) E_n^{\mathrm{OCM}} (\psi_n|\right] = \sum_n f_n(\mu) E_n^{\mathrm{OCM}}. \tag{30}$$

By using the partial trace of Eq. (30), the local energy can be defined as

$$\langle E\rangle_A \equiv \mathrm{Tr}_A[H_0\rho] = \mathrm{Tr}_A\left[\sum_n |\psi_n) f_n(\mu) E_n^{\mathrm{OCM}} (\psi_n|\right] = \sum_n f_n(\mu) w_n^A E_n^{\mathrm{OCM}}. \tag{31}$$

Since $f_n(\mu)$ and w_n^A are real numbers, the real and imaginary parts of $\langle E\rangle_A$ should be interpreted as the energy and the energy width of the subsystem A, respectively. Therefore, the electron-transfer (ET) rate from the subsystem A to the remaining part of the model cluster, $\kappa_{\mathrm{ET}}^A(\mu)$, can be evaluated by

$$\kappa_{\mathrm{ET}}^A(\mu) = -2\,\mathrm{Im}\langle E\rangle_A = \sum_n f_n(\mu) w_n^A \gamma_n. \tag{32}$$

It should be noted that there is no net electron transfer in an equilibrium condition, and thus, the rate of the reverse process, i.e., the electron transfer from the surface to the adsorbate, is required to be equal to $\kappa_{\mathrm{ET}}^A(\mu)$. If an electronic excitation locally occurs on the adsorbate region described by the model cluster, the chemical potential of the adsorbate region is changed from the equilibrium value μ_{eq} to a different one μ^*, whereas that of the bulk environment remains to be μ_{eq}. The imbalance of the chemical potentials causes net electron transfer between the adsorbate and the surface. The rate is given by

$$k_{\mathrm{ET}}^A(\mu^*, \mu_{\mathrm{eq}}) \equiv \kappa_{\mathrm{ET}}^A(\mu^*) - \kappa_{\mathrm{ET}}^A(\mu_{\mathrm{eq}}) = \sum_n \Delta f_n w_n^A \gamma_n, \tag{33}$$

where $\Delta f_n \equiv f_n(\mu^*) - f_n(\mu_{\mathrm{eq}})$ is difference in the occupation numbers for μ^* and μ_{eq}.

B. Adsorption-distance dependence of total and local density of states

Figure 4 shows the adsorption-distance (R) dependence of the total OCM-DOS (blue) and the OCM-LDOS of the adsorbate (red) calculated from Eqs. (17) and (24), respectively, where $E_n^{\mathrm{OCM}} = \epsilon_n - i\gamma_n/2$ is obtained by diagonalizing the complex-scaled Hamiltonian matrix of Eq. (19). The gray-colored array of δ functions in this figure represents the total CCM-DOS similarly calculated from Eq. (13), where E_n^{CCM} is obtained by diagonalizing the Hamiltonian matrix of Eq. (19). Figure 4(a) shows these DOSs at $R=5$. The LDOS is well separated from the surface DOS and energetically localized because the interaction between the adsorbate and the surface is weak. The CCM also gives the correct spectrum position of the adsorbate as indicated by the arrow. This regime ($R=5$) can be regarded as the perturbative one. The adsorbate-surface interaction becomes stronger and the LDOS comes to be energetically delocalized with decreasing the adsorption distance [$R=4$, Fig. 4(b)]. The peak positions of the CCM and the OCM are different from each other. In this regime, the CCM is no longer able to describe the accurate DOS. The LDOS consists of two energetically localized peaks with further decreasing the adsorption distance [$R=3$, Fig. 4(c)]. The two peaks correspond to the adsorbate-surface bonding and antibonding energy levels. Since their wave functions are spatially localized in the vicinity of the adsorbate, the CCM also gives the reasonable peak positions for these two energy levels as denoted by the two arrows. The above behavior of the R dependence of the LDOS with the OCM is consistent with the standard model of chemisorption by Newns.[66] In contrast, the CCM gives an accurate description of the local properties only for limited R. For these reasons, it is concluded that the introduction of the OCM is indispensable for the unified description of adsorbate-surface systems.

C. Comparison of chemical bonding in conventional cluster model and open-boundary cluster model

We shall discuss differences in the nature of chemical bonding described with the CCM and the OCM. To evaluate the total and adsorption energies, we have to specify the electronic configuration of the system. The electronic configurations are determined by giving the total number of electrons for the CCM and the Fermi energy for the OCM. We adopt an adsorbate-surface model system consisting of 11 surface electrons (i.e., one electron per surface atom) and two adsorbate electrons in the CCM. For $R=\infty$, the two lowest-lying adsorbate one-body energy levels are at $E=-3.27$ and -1.21, and the lowest surface energy band is lying in the region of $E=-1.43$ to -1.14. We thus set the Fermi energy to be -1.3 in the OCM so that the electronic configuration of the OCM coincides with that of the CCM at $R=\infty$. Figure 5 shows the R dependence of the local energy for different choices of the subspace A, computed by using Eq. (31) for the OCM and the corresponding definition for the CCM,

$$\langle E\rangle_A^{\mathrm{CCM}} = \mathrm{Tr}_A[H\rho] = \sum_n f_n^{\mathrm{CCM}} w_n^{A,\mathrm{CCM}} E_n^{\mathrm{CCM}}, \tag{34}$$

where f_n^{CCM} and E_n^{CCM} are the integer occupation number and the one-body energy of the CCM, respectively, and $w_n^{A,\mathrm{CCM}}$ is given by

$$w_n^{A,\mathrm{CCM}} = \int_{x\subset A} |\psi_n^{\mathrm{CCM}}(x)|^2 dx. \tag{35}$$

The symbol $\langle E\rangle_n$ indicates the local energy for the subspace consisting of the adsorbate atom and the n local atoms extracted from the 11-atom surface model cluster. The R dependence of the total energy denoted by $\langle E\rangle_{11}$ is also shown. The origin of the energy is defined as the asymptotic ($R\to\infty$) value of $\langle E\rangle_A$. The most striking difference between the CCM and OCM results is how the local-energy curve depends on the choice of the subspace. The OCM local-energy curves are almost independent of the subspace, whereas the CCM ones strongly depend on it.

To understand the reason for the local-energy difference depending on the subspace, we introduce the 1-RDM in the real space,

$$\rho(x',x) = (x'|\rho|x) = \sum_n f_n \phi_n(x')\phi_n(x). \tag{36}$$

This quantity is very useful because the off-diagonal part of the 1-RDM is known to be related to the property of chemical bonding. The Mulliken's overlap population is an index for chemical bonding and nothing but the off-diagonal part of the 1-RDM in an atomic orbital representation.[67] Moreover, $\rho(x',x)$ is related to the first-order correlation function of an electron quantum field $G^{(1)}(x,x')$,

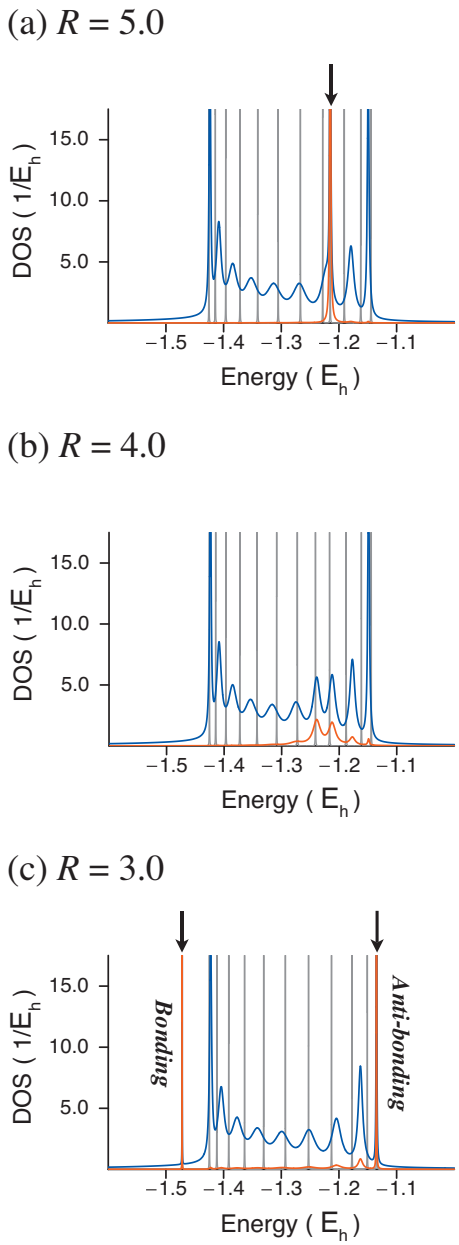

FIG. 4. (Color) Adsorption-distance dependence of the one-electron total DOS (blue) and local DOS (red) calculated with the OCM. The gray-colored array of δ functions represents the one-electron total DOS obtained with the CCM. The arrows indicate the CCM peak positions representing the states localized on the adsorbate.

$$G^{(1)}(x,x') \equiv \langle \hat{\psi}^{\dagger}(x)\hat{\psi}(x')\rangle = \rho(x',x), \tag{37}$$

where $\hat{\psi}^{\dagger}(x)$ and $\hat{\psi}(x')$ are creation and annihilation operators of the electron quantum field at the positions of x' and x, respectively. As in the context of quantum optics,[68] the correlation function $G^{(1)}(x,x')$ gives an extent of interference (i.e., coherence) between particles at x and x'.[69] We can therefore investigate chemical bonding from the viewpoint of the electron coherence by analyzing the real-space 1-RDM. Mukamel *et al.* employed such an analysis at the level of a

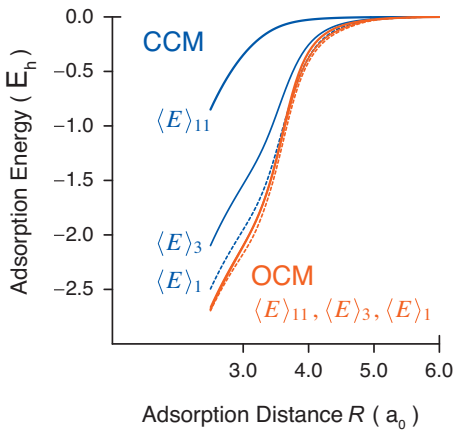

FIG. 5. (Color) Adsorption-distance dependence of the local and total energies obtained with the CCM (blue) and the OCM (red). The chemical potential is set to be −1.3.

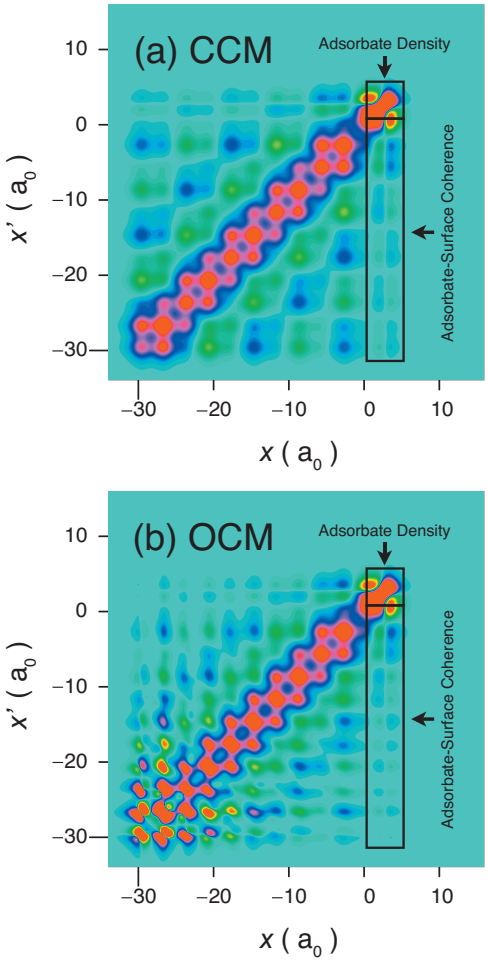

FIG. 6. (Color) One-body reduced density matrix in the real-space representation obtained with (a) CCM and (b) OCM. The adsorbate density and the adsorbate-surface coherence are illustrated in the square and rectangle regions, respectively. The adsorption distance and the chemical potential are set to be 2.5 and −1.3, respectively.

coarse-grained atomic orbital representation to investigate nonlinear optical responses of molecules.[70]

Figure 6 shows the real-space representation of the 1-RDMs for the CCM and the OCM. Our interest is in the adsorbate-surface chemical bond, and thus, we concentrate on the region indicated by the rectangles in the figure. It is clearly shown in Fig. 6 that each attenuation length of the adsorbate coherence, referred to as the coherence length, is different in the CCM and the OCM. The coherence remains even at the edge of the model cluster (i.e., large x and small x' and vice versa) in the CCM, whereas it does not in the OCM. In other words, the coherence length in the OCM is shorter than that in the CCM. This is the reason that the local-energy curves for the OCM in Fig. 5 do not depend on the choice of the subspace. The coherence length in the CCM is always equal to the size of the model cluster because there exist reflection waves from the edge of the cluster. This leads to an artificial edge effect causing a numerically slow size convergence. It is difficult to remove such an edge effect in the CCM with a systematic prescription. On the other hand, the artificial coherence occurred in the CCM is circumvented by employing the OBC in the OCM, and indeed, the OCM gives the proper description of the adsorbate-surface system. The physical properties of the adsorbate are essentially independent of the cluster size in the OCM if the cluster size is larger than the size associated with the adsorbate coherence length. The CCM apparently overestimates the coherence length in the adsorbate-surface system. The OCM results demonstrate that the chemisorption is a local phenomenon. This conclusion is well consistent with chemists' intuition.

IV. APPLICATION TO ADSORBATE DYNAMICS INDUCED BY CHANGING CHEMICAL POTENTIAL

A. Global and local changes of chemical potential

We have discussed above the equilibrium properties of DOS and chemical bonding in the adsorbate-surface system modeled by the OCM approach. On the other hand, adsorbate dynamics is generally triggered by changing a chemical potential μ. The definition of the occupation number of Eq. (29) allows us to investigate μ dependent properties of the system. It should be noted that there are two ways of changing the chemical potential: a global change and a local change. When the chemical potential is globally changed in the whole system, the equilibrium is maintained between the adsorbate region, which is explicitly described with the model cluster, and the environment. In this case, no net ET occurs, as mentioned in Sec. III A. Thus, the global change of μ only affects the adsorbate-surface interaction through a change of $\mathrm{Re}[\langle E\rangle]$. The global change of μ is relevant in, for example, electrode reactions induced by applying bias voltage. If the chemical potential is locally changed in the adsorbate region, a net electron transfer associated with $\mathrm{Im}[\langle E\rangle]$ occurs in addition to change of the adsorbate-surface interaction. The net ET is induced by imbalanced chemical potentials between the adsorbate region (μ^*) and the environment (μ_{eq}), and thus, its rate is given by Eq. (33). The local change of the chemical potential plays an important role in, for example, indirect desorption induced by electronic transition (DIET), which is typically observed in adsorbate-metallic surface systems. As reviewed by Saalfrank,[71] photoexcitation of those systems generally causes indirect photodesorptions. The photon energy is injected not to the adsorbate but to the surface at first, and subsequent energy transfer occurs from the surface to the adsorbate. As a result, the local chemical potential in the adsorbate region becomes higher than it was in equilibrium, and then the adsorbate desorbs. The rate of co-occurring electronic relaxation is known to be a key factor in determining the desorption probability.[72,73]

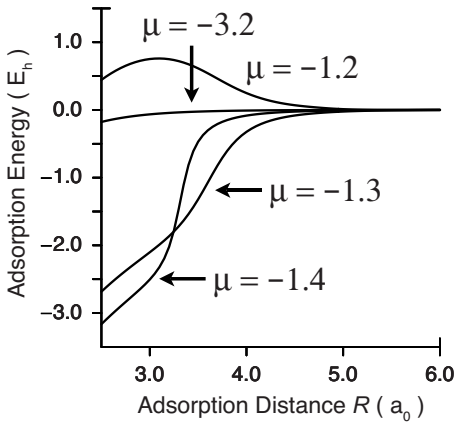

FIG. 7. Chemical potential dependence of the adsorption energy curves.

In summary, the adsorbate-surface interaction is altered by both types of changes of μ, whereas the net ET from the adsorbate to the surface is induced only by local change of μ. We shall investigate the former in Sec. IV B and the latter in Sec. IV C, separately.

B. Chemical potential dependence of adsorption energy

Figure 7 shows the R dependence of the interaction energy $\langle E\rangle_{11}^{\mathrm{OCM}}$ for different values of μ. We see that the potential energy which is felt by nuclei strongly depends on the chemical potential of the adsorbate region. The curve for $\mu=-3.2$ illustrates that the adsorbate atom has almost no interaction with the surface. This is because the occupied orbital is only the lowest one-body energy level that is always localized on the adsorbate atom. When the chemical potential is set equal to the energies in the surface electronic band ($E=-1.43$ to -1.14), the adsorbate interacts with the surface. Indeed, the interaction is attractive for $\mu=-1.4$ and -1.3. When $\mu=-1.2$, the adsorbate energy level and the surface electronic band are almost fully occupied at the asymptotic R. Then, the interaction between the adsorbate and the surface becomes repulsive for large R ($\geqslant 3.2$), as shown in Fig. 7.

C. Electron transfer induced by local electronic excitation

As explained in Sec. IV A, adsorbate dynamics induced by a local electronic excitation such as indirect DIET in-

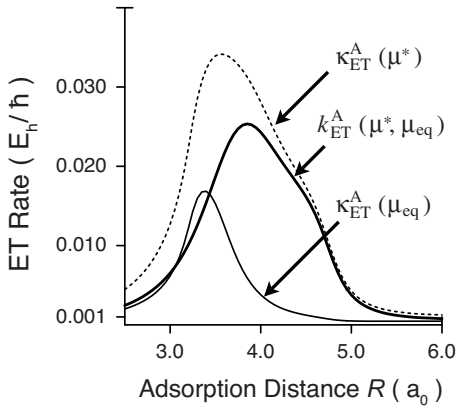

FIG. 8. Comparison of the adsorption-distance dependence of the ET rate from the adsorbate to the surface. The bold curve shows the net ET rate obtained by Eq. (33) for the locally excited state of $\mu^*=-1.2$. The equilibrium chemical potential is taken to $\mu_{eq}=-1.3$. The net ET rate is equal to the difference of the rates obtained by Eq. (32) for $\mu=-1.3$ (thin curve) and -1.2 (dotted-thin curve).

volves not only change of the potential energy curve but also co-occurring electronic relaxation, originating from the electron transfer from the adsorbate to the surface. We shall here evaluate the rate of the electron transfer. To simulate an indirect DIET process, we use a set of parameters to specify the model as follows. The chemical potential of the model cluster is set to be -1.3 in equilibrium ($=\mu_{eq}$) and then changed to be -1.2 ($=\mu^*$) by the local electronic excitation. The Hamiltonian of Eq. (19) has a continuous electronic band in the energy range of $E=-1.43$ to -1.14, and thus, the model cluster describes properties of the adsorbate interacting with a metallic surface by taking $\mu_{eq}=-1.3$. Figure 8 shows the net electron-transfer rate (bold curve) induced by the local electronic excitation from equilibrium to the excited adsorbate state. The rate was calculated through Eq. (33) using the R-dependent rate for $\mu_{eq}=-1.3$ (thin curve) and $\mu^*=-1.2$ (dotted-thin curve). For a large adsorption distance R, both the rates for μ_{eq} and μ^* are small because the interaction between the adsorbate and the surface is weak. As the adsorption distance R decreases, the rates gradually increase owing to the strong interaction. The rates have each maximum value and then monotonically decrease again for $R<3.4$. This behavior is clarified by analyzing the R dependence of the LDOS, as shown in Fig. 4. As described in Sec. III B, the LDOS consists of the energetically localized two peaks and their corresponding wave functions are spatially localized in the vicinity of the adsorbate at $R\lesssim 3.5$. The decrease in these ET rates is ascribed to the localization of the wave functions. As a result, the net ET rate has a maximum at $R\simeq 4.0$. The system feels the potential of the electronically excited state only during the time scale of the inverse ET rate. Therefore, the rate and its R dependence are of a crucial importance for discussing photoinduced dynamics on adsorbate-metallic surface systems. As understood from the expression of Eq. (33), the ET rate is always zero when the eigenvalues of Hamiltonian are real, and thus, the CCM gives no information on dynamics related to the electronic relaxation. We conclude that the OCM approach is promising for describing dynamics of adsorbate-metallic surface systems.

V. APPLICABILITY OF OPEN-BOUNDARY CLUSTER MODEL TO REAL SYSTEM

In the present work, we concentrated on developing the theoretical framework of the OCM approach and illustrated its advantages over other formalisms by using simple model systems. We discuss here the applicability of the OCM approach to real systems. Although the complex-scaling technique, which is used to apply the OBC to the system, requires dilatation analyticity of Hamiltonian, its property is generally not satisfied by the Hamiltonian of a model cluster of an adsorbate-surface system. However, the alternative approach called the complex basis function method has been proposed[74–76] in the form applicable to *ab initio* molecular Hamiltonians and successfully applied[59,77,78] to electronic resonance states in real systems. Thus, there are, in principle, no difficulties in applying the OCM approach to adsorbate-surface Hamiltonians. We remark that complex-valued orbital exponents used in the complex basis function method must be carefully selected because the complex variational principle is only a stationary principle.[79] The basis-set dependence of the OCM results for real systems should be extensively investigated. If this problem is solved, the OCM approach becomes really promising. It should be further noted that this method can be straightforwardly extended to many-body formalisms as have been done in molecular electronic resonance problems,[59,77,78] and thus, it is possible to directly calculate electronically excited states of adsorbate-surface systems with the OCM approach.

VI. CONCLUDING REMARKS

We have proposed a cluster model, OCM, to describe adsorbate-surface systems. This model is based on the philosophy of the Löwdin-Feshbach partition approach. The philosophy is that the subsystem should be extracted as an open-quantum system. To practically realize such an extraction of the subsystem, we introduced the model cluster with the proper OBC. The divergence of the wave functions induced by the introduction of the OBC is circumvented by using the complex-scaling technique. The OBC removes the edge effect caused by the waves reflected at the edge of the model cluster. As a result, the OCM gives appropriate continuous DOS. It is explicitly shown by analyzing off-diagonal elements of 1-RDM in the real-space representation that the CCM suffers from an artificial coherence due to the edge effect. On the other hand, the OCM is free from the edge effect and thus reasonably describes a coherence in the adsorbate-surface system. Indeed, the correct adsorption energy can be calculated with a small-size cluster in the OCM. In contrast to the CCM, the OCM allows us to estimate the electron-transfer rate from the adsorbate to the surface by using the imaginary parts of the adsorbate one-body energies. This aspect is important in discussing photoinduced dynamics of adsorbate-metallic surface systems. It should also

be stressed that we can intuitively analyze the properties of the semi-infinite system in terms of the local picture inherent in the OCM approach. The OCM approach is expected to be straightforwardly applied to real systems by employing the complex basis function method and will be a computationally less demanding tool to investigate properties and dynamics of adsorbate-surface systems.

ACKNOWLEDGMENTS

The present work was supported by Grant-in-Aid (Nos. 18066019 and 19750013) and by the Next Generation Super Computing Project, Nanoscience Program, from the Ministry of Education, Culture, Sports, Science and Technology of Japan.

*Corresponding author. nobusada@ims.ac.jp

[1] N. B. Hannay, *Treatise on Solid State Chemistry* (Plenum Press, New York, 1976), Pts. 6A and 6B.
[2] E. Drauglis, R. D. Gretz, and R. I. Jaffe, *Molecular Processes on Solid Surface* (McGraw-Hill, New York, 1969).
[3] G. Binnig, H. Rohrer, Ch. Gerber, and E. Weibel, Phys. Rev. Lett. **49**, 57 (1982).
[4] B. C. Stipe, M. A. Rezaei, and W. Ho, Science **280**, 1732 (1998).
[5] J. I. Pascual, J. J. Jackiw, Z. Song, P. S. Weiss, H. Conrad, and H.-P. Rust, Phys. Rev. Lett. **86**, 1050 (2001).
[6] T. Komeda, Y. Kim, M. Kawai, B. N. J. Persson, and H. Ueba, Science **295**, 2055 (2002).
[7] H. Petek, M. J. Weida, H. Nagano, and S. Ogawa, Science **288**, 1402 (2000).
[8] K. Watanabe, N. Takagi, and Y. Matsumoto, Phys. Rev. Lett. **92**, 057401 (2004).
[9] X.-Y. Zhu, Annu. Rev. Phys. Chem. **53**, 221 (2002).
[10] G. P. Brivio and M. I. Trioni, Rev. Mod. Phys. **71**, 231 (1999).
[11] E. Wimmer, A. J. Freeman, J. R. Hiskes, and A. M. Karo, Phys. Rev. B **28**, 3074 (1983).
[12] L. A. Hemstreet, S. R. Chubb, and W. E. Pickett, Phys. Rev. B **40**, 3592 (1989).
[13] H. Ishida and K. Terakura, Phys. Rev. B **40**, 11519 (1989).
[14] Y. Miyamoto and A. Oshiyama, Phys. Rev. B **41**, 12680 (1990).
[15] K. C. Hass, M.-H. Tsai, and R. V. Kasowski, Phys. Rev. B **53**, 44 (1996).
[16] J. A. White, D. M. Bird, and M. C. Payne, Phys. Rev. B **53**, 1667 (1996).
[17] V. Pallassana, M. Neurock, L. B. Hansen, B. Hammer, and J. K. Nørskov, Phys. Rev. B **60**, 6146 (1999).
[18] M. P. de Lara-Castells and J. L. Krause, J. Chem. Phys. **115**, 4798 (2001).
[19] S. Yanagisawa, T. Tsuneda, K. Hirao, and Y. Matsuzaki, J. Mol. Struct.: THEOCHEM **716**, 45 (2005).
[20] Y. Cao and Z.-X. Chen, Surf. Sci. **600**, 4572 (2006).
[21] *Cluster Models for Surface and Bulk Phenomena*, edited by G. Pacchioni, P. S. Bagus, and F. Parmigiani, NATO ASI, Series B: Physics (Plenum, New York, 1992), Vol. 283.
[22] K. Hermann, P. S. Bagus, C. R. Brundle, and D. Menzel, Phys. Rev. B **24**, 7025 (1981).
[23] M. W. Ribarsky, W. D. Luedtke, and U. Landman, Phys. Rev. B **32**, 1430 (1985).
[24] P. S. Bagus and G. Pacchioni, J. Chem. Phys. **102**, 879 (1995).
[25] A. Redondo, W. A. Goddard III, T. C. McGill, and G. T. Surratt, Solid State Commun. **20**, 733 (1976).
[26] P. Nachtigall, K. D. Jordan, and K. C. Janda, J. Chem. Phys. **95**, 8652 (1991).
[27] R. Konecny and D. J. Doren, Surf. Sci. **417**, 169 (1998).
[28] T. Klüner, H.-J. Freund, J. Freitag, and V. Staemmler, J. Chem. Phys. **104**, 10030 (1996).
[29] I. V. Yudanov, V. A. Nasluzov, K. M. Neyman, and N. Rosch, Int. J. Quantum Chem. **65**, 975 (1997).
[30] M. Chiesa, E. Giamello, C. Di Valentin, G. Pacchioni, Z. Sojka, and S. Van Doorslaer, J. Am. Chem. Soc. **127**, 16935 (2005).
[31] H. Nakatsuji and H. Nakai, J. Chem. Phys. **98**, 2423 (1993).
[32] J. L. Whitten and T. A. Pakkanen, Phys. Rev. B **21**, 4357 (1980).
[33] J. L. Whitten, Phys. Rev. B **24**, 1810 (1981).
[34] H. Yang and J. L. Whitten, J. Am. Chem. Soc. **113**, 6442 (1991).
[35] H. A. Duarte and D. R. Salahub, J. Chem. Phys. **108**, 743 (1997).
[36] P. Cortona, Phys. Rev. B **44**, 8454 (1991).
[37] N. Govind, Y. A. Wang, A. J. R. da Silva, and E. A. Carter, Chem. Phys. Lett. **295**, 129 (1999).
[38] T. Klüner, N. Govind, Y. A. Wang, and E. A. Carter, J. Chem. Phys. **116**, 42 (2002).
[39] P. Huang and E. A. Carter, J. Chem. Phys. **125**, 084102 (2006).
[40] P. O. Löwdin, J. Math. Phys. **3**, 969 (1962).
[41] H. Feshbach, Ann. Phys. (N.Y.) **5**, 357 (1958).
[42] T. B. Grimley and C. Pisani, J. Phys. C **7**, 2831 (1974).
[43] A. R. Williams, P. J. Feibelman, and N. D. Lang, Phys. Rev. B **26**, 5433 (1982).
[44] T. Klamroth and P. Saalfrank, Surf. Sci. **410**, 21 (1998).
[45] J. E. Inglesfield, J. Phys. C **14**, 3795 (1981).
[46] J. E. Inglesfield and G. A. Benesh, Phys. Rev. B **37**, 6682 (1988).
[47] W. P. Reinhardt, Annu. Rev. Phys. Chem. **33**, 233 (1982); C. W. McCurdy, in *Resonances in Electron-Molecule Scattering, van der Waals Complexes, and Reactive Chemical Dynamics*, edited by D. G. Truhlar (American Chemical Society, Washington, DC, 1984), Vol. 263, p. 17; N. Moiseyev, Phys. Rep. **302**, 211 (1998).
[48] N. Moiseyev, T. Maniv, R. Elber, and R. B. Gerber, Mol. Phys. **55**, 1369 (1985); U. Peskin and N. Moiseyev, J. Chem. Phys. **96**, 2347 (1992); **97**, 2804 (1992); Int. J. Quantum Chem. **46**, 343 (1993).
[49] P. Nordlander and J. C. Tully, Phys. Rev. Lett. **61**, 990 (1988).
[50] P. Nordlander and J. C. Tully, Phys. Rev. B **42**, 5564 (1990).
[51] R. D. Levine, *Quantum Mechanics of Molecular Rate Processes* (Oxford University Press, London, 1969).
[52] F. Coester and H. Kümmel, Nucl. Phys. **9**, 225 (1958–59).
[53] J. Okolowicz, M. Ploszajczak, and I. Rotter, Phys. Rep. **374**, 271 (2003).
[54] J. Humblet and L. Rosenfeld, Nucl. Phys. **26**, 529 (1961).
[55] R. Id Betan, R. J. Liotta, N. Sandulescu, and T. Vertse, Phys. Rev. Lett. **89**, 042501 (2002).
[56] N. Michel, W. Nazarewicz, M. Ploszajczak, and K. Bennaceur, Phys. Rev. Lett. **89**, 042502 (2002).
[57] V. F. Weisskopf and E. Wigner, Z. Phys. **63**, 54 (1930).

[58] A. J. F. Siegert, Phys. Rev. **56**, 750 (1939).
[59] T. Yasuike and S. Yabushita, Chem. Phys. Lett. **316**, 257 (2000).
[60] T. Yasuike and K. Someda, Phys. Rev. A **66**, 053410 (2002).
[61] D. T. Colbert and W. H. Miller, J. Chem. Phys. **96**, 1982 (1992).
[62] C. Y. Yang, K. H. Johnson, D. R. Salahub, J. Kaspar, and R. P. Messmer, Phys. Rev. B **24**, 5673 (1981).
[63] K. Lee, J. Callaway, and S. Dhar, Phys. Rev. B **30**, 1724 (1984).
[64] N. D. Lang and W. Kohn, Phys. Rev. B **1**, 4555 (1970).
[65] T. Berggren, Phys. Lett. **33B**, 547 (1970).
[66] D. M. Newns, Phys. Rev. **178**, 1123 (1969).
[67] R. S. Mulliken, J. Chem. Phys. **23**, 1833 (1955).
[68] J. R. Klauder and E. C. G. Sudarshan, *Fundamentals of Quantum Optics* (Benjamin, New York, 1968); R. J. Glauber, Phys. Rev. **130**, 2529 (1963).
[69] M. Naraschewski and R. J. Glauber, Phys. Rev. A **59**, 4595 (1999).
[70] S. Mukamel, A. Takahashi, H. X. Wang, and G. Chen, Science **266**, 250 (1994).
[71] P. Saalfrank, Chem. Rev. (Washington, D.C.) **106**, 4116 (2006).
[72] P. Saalfrank, G. Boendgen, K. Finger, and L. Pesce, Chem. Phys. **251**, 51 (2000).
[73] A. Abe and K. Yamashita, J. Chem. Phys. **119**, 9710 (2003).
[74] C. W. McCurdy and T. N. Rescigno, Phys. Rev. Lett. **41**, 1364 (1978).
[75] N. Moiseyev and C. T. Corcoran, Phys. Rev. A **20**, 814 (1979).
[76] C. W. McCurdy, Phys. Rev. A **21**, 464 (1980).
[77] J. F. McNutt and C. W. McCurdy, Phys. Rev. A **27**, 132 (1983).
[78] S. Yabushita and C. W. McCurdy, J. Chem. Phys. **83**, 3547 (1985).
[79] D. G. Truhlar and C. A. Mead, Phys. Rev. A **42**, 2593 (1990).